THE BEHAVIOR OF ELASTIC WAVES NEAR A FREE BOUNDARY

By

PHILIP WAYNE RANDLES

Bachelor of Science

Oklahoma State University of Agriculture and Applied Science

Stillwater, Oklahoma

1962

Submitted to the Faculty of the Graduate School of
the Oklahoma State University of Agriculture and
Applied Science in partial fulfillment of the
requirements for the degree of
MASTER OF SCIENCE
August, 1963

THE BEHAVIOR OF ELASTIC WAVES

NEAR A FREE BOUNDARY

Thesis Approved:

Richard L. Lowery
Thesis Adviser

Ladislaus J. Fila

James Maddox
Dean of the Graduate School

PREFACE

Elastic waves in solids have been of interest for many years mainly because they are the mechanism by which the energy of an earthquake is propagated. More recently they have been applied in seismic testing for earth formations and deposits. Elastic waves in the ultrasonic frequency range are now being used for flaw testing in many materials. These waves have a short wave length and the capability of resolving very small flaws.

The refraction of an elastic wave at a solid-solid interface presents the problem of how a wave will behave in the transition between the critical angle, where the wave propagates along the surface of one of the solids, and an angle which refracts the wave into the second solid.

The purpose of this study is to try to locate an elastic wave in this transition region between a surface wave and an internal wave and to study its behavior. The mathematical description of this problem resolves into a very interesting and challenging set of equations and boundary conditions.

Appreciation is expressed to Dr. R. L. Lowery, for suggestions and encouragement during this study; to Frank Kay, Jesse McIlhaney, Paula Vanhooser and Jerry Whitehouse, for taking data and preparing drawings; to Lael Benjamin and George Cooper for the machine work which aided this investigation; and to Mrs. Bob Schenandoah for typing the manuscript.

TABLE OF CONTENTS

LIST OF FIGURES

CHAPTER I

INTRODUCTION

This problem of how an elastic wave would behave near a free boundary originated from a proposed method of measuring surface fatigue flaw depth by using a shear wave beam aimed near the surface. The shear wave would be aimed so as to skim very close under the surface of the material and reflect when it struck a fatigue flaw as shown in Figure 1.

This method would require that a sizeable portion of the energy could be concentrated into a narrow, straight beam shear wave. These requirements immediately presented the question of whether or not a shear wave would continue to travel in a straight path when in a region near a free boundary. A free boundary will not support normal or shearing stress at the boundary surface.

A shear wave is conveniently produced in a steel bar by an incident longitudinal (compressive) wave passing through a plastic material in contact with the steel. The longitudinal wave is refracted at the interface and a shear wave is produced in the steel. Snell's law of refraction, as given by Redwood (1)[1], which related the velocity and angle of the incident wave to the velocity and angle of refracted wave, is given in

---

[1]Numbers in parentheses refer to sources listed in the Selected Bibliography.

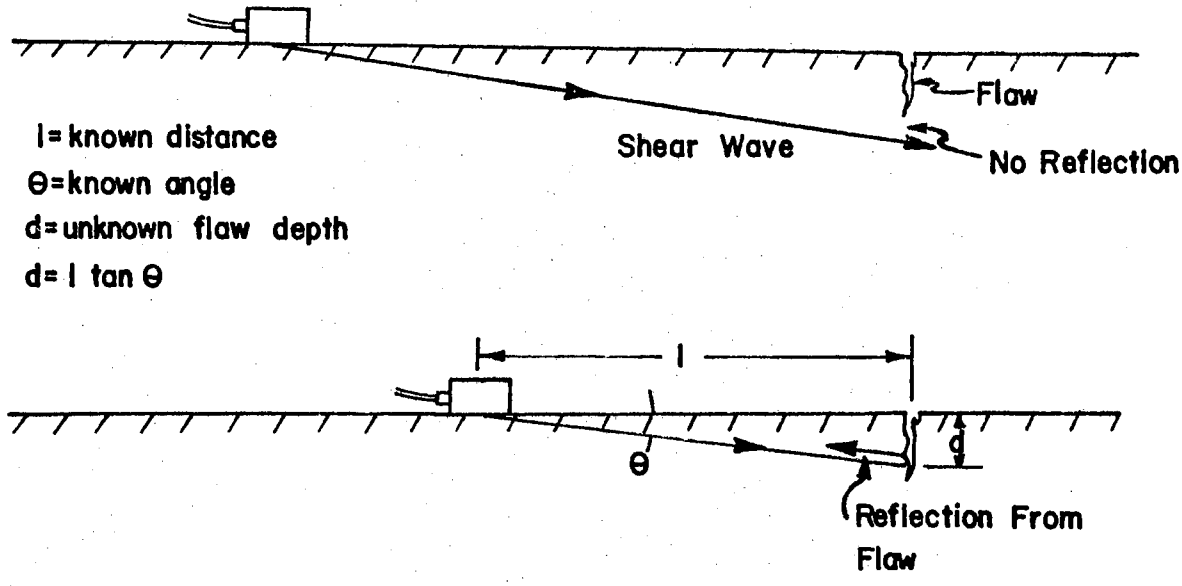

Figure 1. Method of Measuring Flaw Depth

Equation (1-1) below. Refraction of the beam is shown in Figure 2 for various different incident angles.

$$\frac{c_l}{\sin\alpha_l} = \frac{c_t}{\sin\alpha_t} \qquad (1\text{-}1)$$

where c_l = velocity of incident longitudinal wave

α_l = angle of incident wave

c_t = velocity of refracted shear wave

α_t = angle of refracted wave

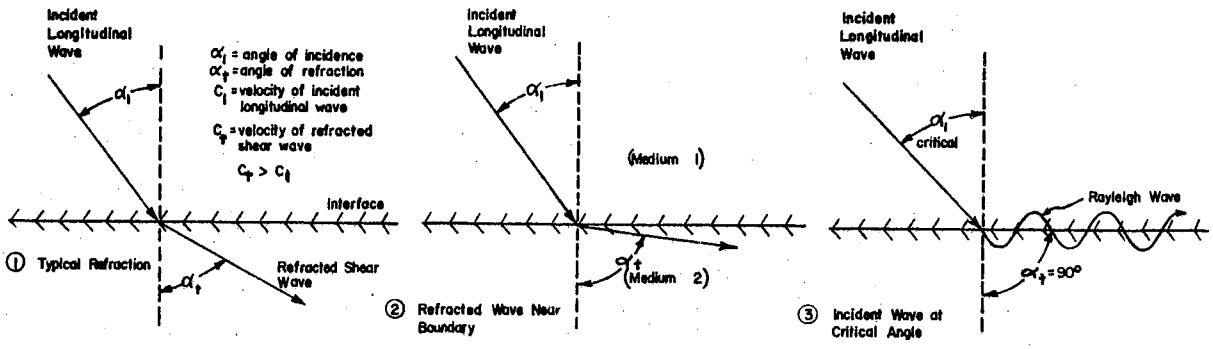

Figure 2. Refraction of Elastic Waves at a Solid-Solid Interface

A variation in the angle of incidence of the incoming longitudinal wave was easily obtained by mounting a straight beam piezoelectric transducer on a Lucite plastic block with a rotating cylindrical base as shown in Figure 3. This design was taken from a similar holder by Rasmussen (2).

Since the longitudinal wave velocity in Lucite is less than the shear wave velocity in steel, the shear wave is refracted further away from the normal than the incident longitudinal wave as shown in Figure 2. This fact makes it possible to adjust the incident wave at a critical angle and produce a Rayleigh surface wave along the interface between the Lucite and steel. The high incidence shear wave should be produced when the angle of incidence is slightly smaller than the critical angle.

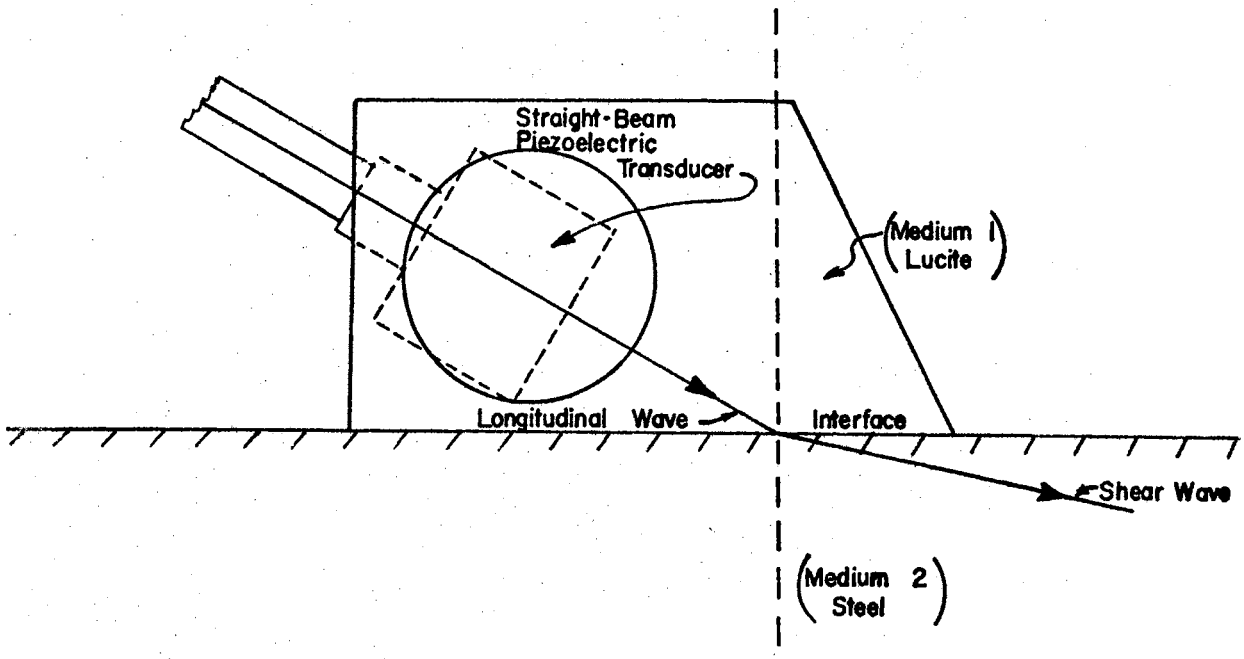

Figure 3. Variable Angle Transducer Holder

Ultrasonic elastic waves are interpreted from a signal, which is picked up by a receiving transducer, amplified and displayed on a screen. The electronic network and schematic of the receiving instrument is explained by Daniel (3) and will not be repeated here.

The signals are interpreted by considering the base line of the signal as time and the ordinate as the amplitude as shown in Figure 4. The output of the transmitter is shown as the initial pulse on the left side of the screen representing zero time, and any signal appearing to the right is from a wave resulting from this output. The distance between the initial pulse and any subsequent signal is directly proportional to the time required for the initial pulse to be transmitted and received again.

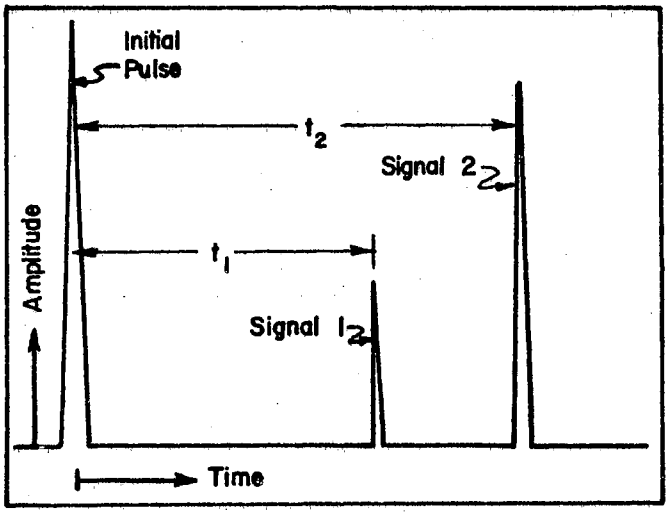

$t_2 > t_1$ indicates it took signal 2 a longer time than signal 1 to reach the receiver.

Figure 4. Typical Screen Picture

CHAPTER II

EXPERIMENTAL OBSERVATIONS

The experimental work consisted of two parts. The first was finding and identifying a signal which was thought to be from a shear wave that was being influenced by the boundary. The second part was determining as much as possible about this wave including the manner and degree in which it was being influenced.

Transmitter-Receiver Setup

The most effective method to detect a signal from an elastic wave is to use a transducer for this purpose alone. Another transducer is used to produce the wave allowing it to travel directly from one transducer to the other without requiring energy losing reflections, which is the case when a single transducer is used both to transmit and receive the wave signal. The use of two separate transducers will be called a transmitter-receiver setup, and this is the arrangement which was used to produce and detect the elastic waves in this investigation.

The transmitter-receiver setup consisted of two straight beam piezoelectric transducers mounted on Lucite plastic blocks (as in Figure 3) so as to give a variation of the angle of incidence for both the transmitter and reciver. The setup is shown in Figure 5.

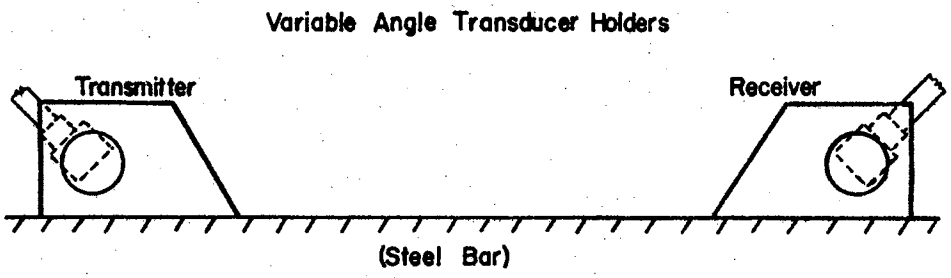

Figure 5. Transmitter - Receiver Setup

The frequency of both transducers was 2.25 MC (megacycles per second) and the material in which the waves were transmitted was a 4-inch square by 18-inch long steel bar.

Dispersion of Beam

The piezoelectric transducers used to produce and receive an ultrasonic elastic wave emit a relatively narrow focused beam; however, it could not be expected that the beam of waves would travel in a coherent path and not disperse to a certain extent. Since this dispersion was present, a beam of elastic waves produced by aiming a transducer in a certain direction was found to be a field of waves with a maximum amplitude occuring in the center of the beam, but with a decreasing amplitude in all directions away from the center. There was never a well defined boundary of the beam as would be expected if dispersion were not present.

Rayleigh Surface Wave Signal

The critical angle at which the maximum Rayleigh surface wave is produced for refraction of a longitudinal wave from Lucite into steel was found to be approximately 66°. It can be seen from Figure 2 that the energy transmitted in this surface wave is made up of that energy which would go into the refracted shear wave if the angle of incidence were decreased. In the transmitter-receiver setup with both angles set at 66°, a large signal was displayed on the screen of the receiver corresponding to the first wave front of Rayleigh surface waves to arrive at the receiver. The surface wave was the first to arrive at the receiver since there were no signals on the screen between the initial pulse and this signal. However, to the right of the first signal was a large number of signals corresponding to trailing surface waves and reflection paths through the plastic block. These trailing waves were of no interest since only the first direct Rayleigh surface wave signal gave any useful information for this arrangement. Since the transmitter-receiver setup was the optimum arrangement for receiving Rayleigh surface waves and the dispersion of the beam was present, a large signal remained on the screen for angles substantially different from 66°.

Identification of Waves

Any wave propagating in the steel bar was easily identified as a surface or internal wave by damping on the surface of the bar. A surface wave signal can be greatly decreased by damping since it is possible for a large portion of the energy to be absorbed. The damping was easily done

by the operator placing his fingers in contact with the surface of the bar between the transmitter and receiver. An internal wave, such as a longitudinal wave or shear wave is unaffected by damping on the surface except at points where the wave reflects from the surface, and damping at these points absorbs a small amount of energy as compared to a surface wave.

The S-wave Signal

When the angles of incidence were decreased, making a shear wave more probable, the surface wave signal was decreased by a large degree, but the signal still remained strong due to the dispersion of the beam described earlier. When the angles were decreased by about 7° from the critical angle of 66°, a small signal appeared on the screen just to the left of the Rayleigh surface wave signal. This signal reached a maximum when both the angle of the transmitter and receiver were adjusted to approximately 57°. This small signal was interpreted to be from a curved shear wave and will be called the S-wave. The reasons for this conclusion will be given in the remainder of this chapter.

The first observation was that the S-wave signal could not be damped at any point on the surface between the transmitter and the receiver and thus was traveling beneath the surface.

The S-wave signal remained a maximum for the angles of incidence adjusted at approximately 57° regardless of the distance between the transmitter and the receiver. This eliminated the possibility that the wave path length was a function of the angle at which it entered the bar.

The fact that the S-wave signal appeared to the left of the surface wave signal, indicated that the S-wave had made the trip between the transmitter and receiver in less time than the surface wave. The ratio of the time required for the S-wave to travel from the transmitter to the receiver to the time required for the Rayleigh surface wave remained approximately constant at 0.92 regardless of the distance between the transmitter and receiver. These signals are shown in Figure 6. This constant ratio indicated that the S-wave and the Rayleigh surface wave were taking approximately the same length path, but the S-wave was traveling at a slightly greater velocity. The paths being of approximately the same length rules out the possiblity that a high velocity longitudinal wave was being reflected from the bottom of the bar. It is well known from Rayleigh (4) and Sokolnikoff (5) that a Rayleigh surface wave in steel travels with a velocity of slightly over nine tenths of the shear wave velocity, which is consistant with the ratio of the times required to travel approximately the same distance.

The S-wave was not present on the surface of the bar, but the path it had taken between the transmitter and receiver was approximately the same as the Rayleigh surface wave path directly along the surface. Therefore, it was concluded that the wave was traveling very near the surface in a curved path as shown in Figure 7.

While damping in the region between the transmitter and receiver did not damp the S-wave signal, it did produce very interesting results. By expanding the range of the receiving instrument, the portion of the signal between the S-wave signal and Rayleigh surface wave signal could

be displayed across the entire screen. Damping on the surface caused a new signal to appear on the screen between the S-wave signal and the Rayleigh surface wave signal which looked similar to the S-wave signal. It required a longer time to reach the receiver than the S-wave signal and a shorter time than the Rayleigh surface wave signal. Further investigation indicated that the wave causing this new signal traveled to the point of damping beneath the surface and continued from that point to the receiver as a Rayleigh surface wave. The point of damping divided the distance between the point of entering at the transmitter and the point of exiting at the receiver into the same ratio as the new signal divided the distance between the Rayleigh surface wave signal and the S-wave signal. This is shown in Figure 8. When the damping was applied very near the receiver, the new signal almost coincided with the S-wave signal. Similarly, when the damping was applied very near the transmitter, the new signal almost coincided with the Rayleigh surface wave signal. The assumed path of the wave causing the new wave is also shown in Figure 8.

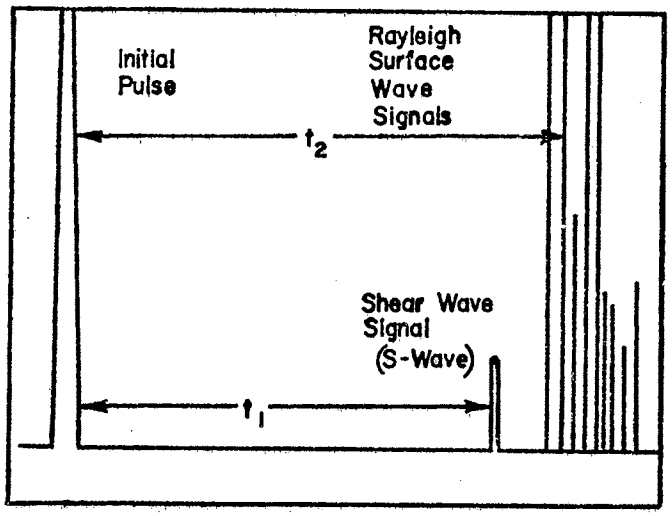

Figure 6. S-Wave Signal on Screen

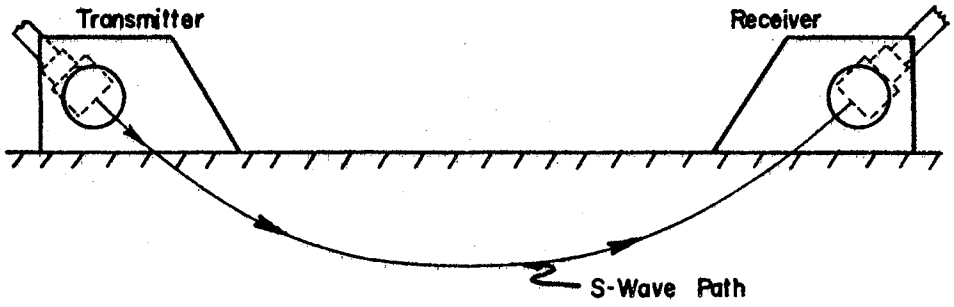

Figure 7. Curved Shear Wave Path

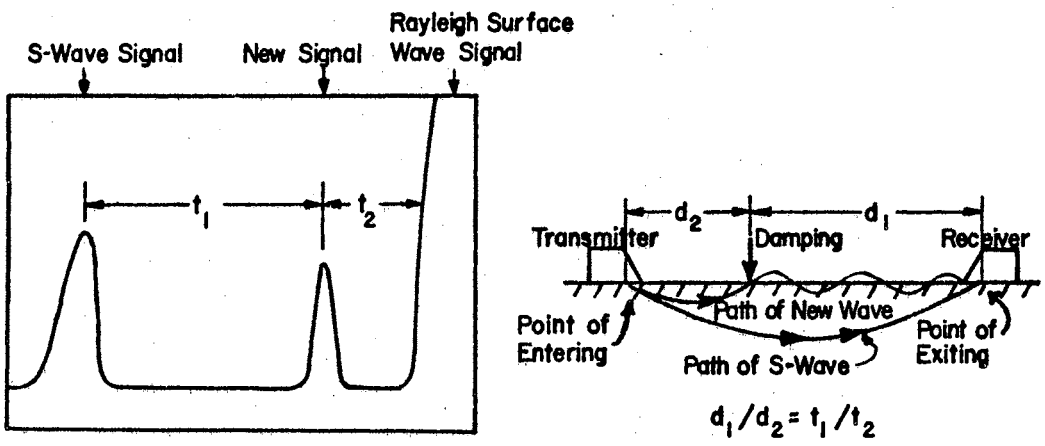

Figure 8. New Signal Caused by Damping

Depth and Shape of S-wave Paths

A true picture of the S-wave paths required knowledge of the depth of the wave beneath the surface which would lead to a plot of the actual shape of the paths. A method was needed to measure the depth of the wave at various points along its path, then the path itself could be plotted.

On preliminary investigation, it was found that a certain thickness of metal was required to support the S-wave. For instance, a signal for the S-wave could not be produced in a $\frac{1}{2}$-inch plate. There were some signals present ahead of the Rayleigh wave signal, but the well defined S-wave signal was not present. The conclusion was that the wave was either being reflected and scattered by the bottom side of the plate or it was being affected equally by the bottom side, since it was also a stress-free surface. A $1\frac{1}{4}$-inch plate would transmit the S-wave signal just as well as the 4-inch bar.

The method used to measure the depth of the S-wave paths consisted of placing an obstruction in the path of the S-wave, thus determining how near the surface of the metal the obstruction could be before the S-wave struck it. The obstruction was a narrow saw cut made from the bottom side of the $1\frac{1}{4}$-inch steel plate. The cut was made with a band saw across the center of the 10 x 16-inch plate and it was made on a taper so that only 1/32-inch of metal was left above the cut on one side and 25/32-inch of metal was left above the cut on the other side as shown in Figure 9. This gave a variable depth of metal without imposing another stress-free boundary near the wave as would be done with just a tapered plate. The top of the plate was ground very smooth to avoid inconsistencies in the readings because of roughness of the surface.

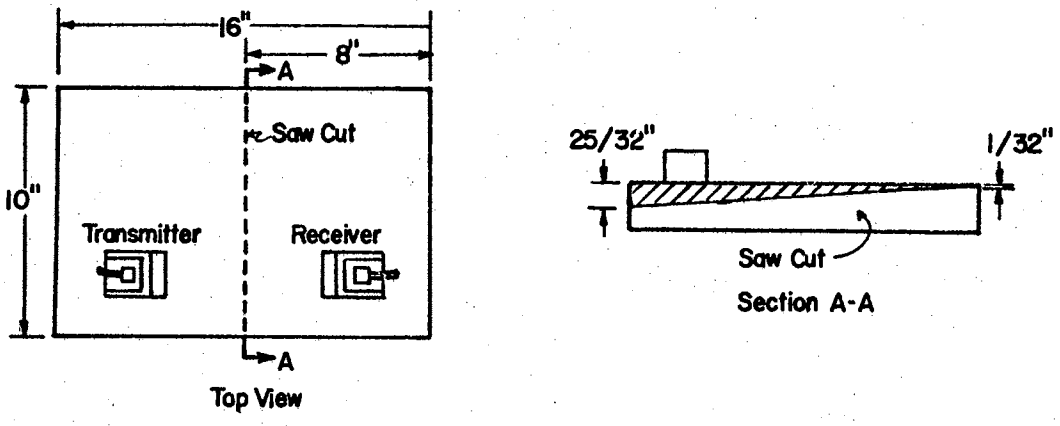

Figure 9. Plate With Tapering Saw Cut

The transmitter and receiver were placed on the top surface so that a line connecting the two and presumably the S-wave path would be perpendicular to the saw cut as shown in Figure 10. By moving the transmitter and receiver laterally across the plate parallel to the saw cut, when the metal above the cut became thinner than the depth of the S-wave path, the signal on the screen would begin to decrease and then disappear completely when it blocked all of the path of the wave (see Figure 10). A set distance between the transmitter and receiver fixed one S-wave path, where one path means the path taken by that portion of the wave which is received by the receiver transducer.

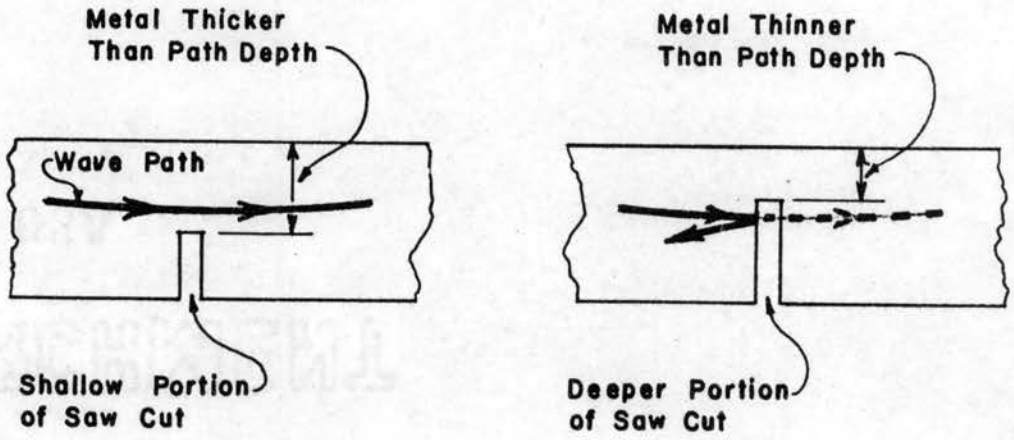

Figure 10. Curved Wave Hitting Saw Cut

A spacer was placed between the transmitter and receiver thus fixing the distance between the point of entering and exiting the metal. For each spacing, readings were taken for various points along the path. The readings were taken by picking a point on the path where the depth was to be determined and moving the transducers laterally so that this point always remained over the saw cut. The amplitude of the signal corresponding to a certain point on the path was recorded for points laterally across the plate. Since the tapered cut was made linear, the lateral distance corresponded directly with a depth of metal above the cut. The amplitude of the received signal was plotted versus the metal depth as in Figure 11. These plots indicated that in the region of the plate where the metal was very thin, no signal was able to get past the cut and as the setup was moved in a direction to increase the depth, some portion

of the signal began to pass over the cut. Through this transition region, the amplitude increased approximately linearly with the increasing metal depth until at a certain depth, all of the wave passed over the cut and no matter how much deeper the metal got, the signal would not increase.

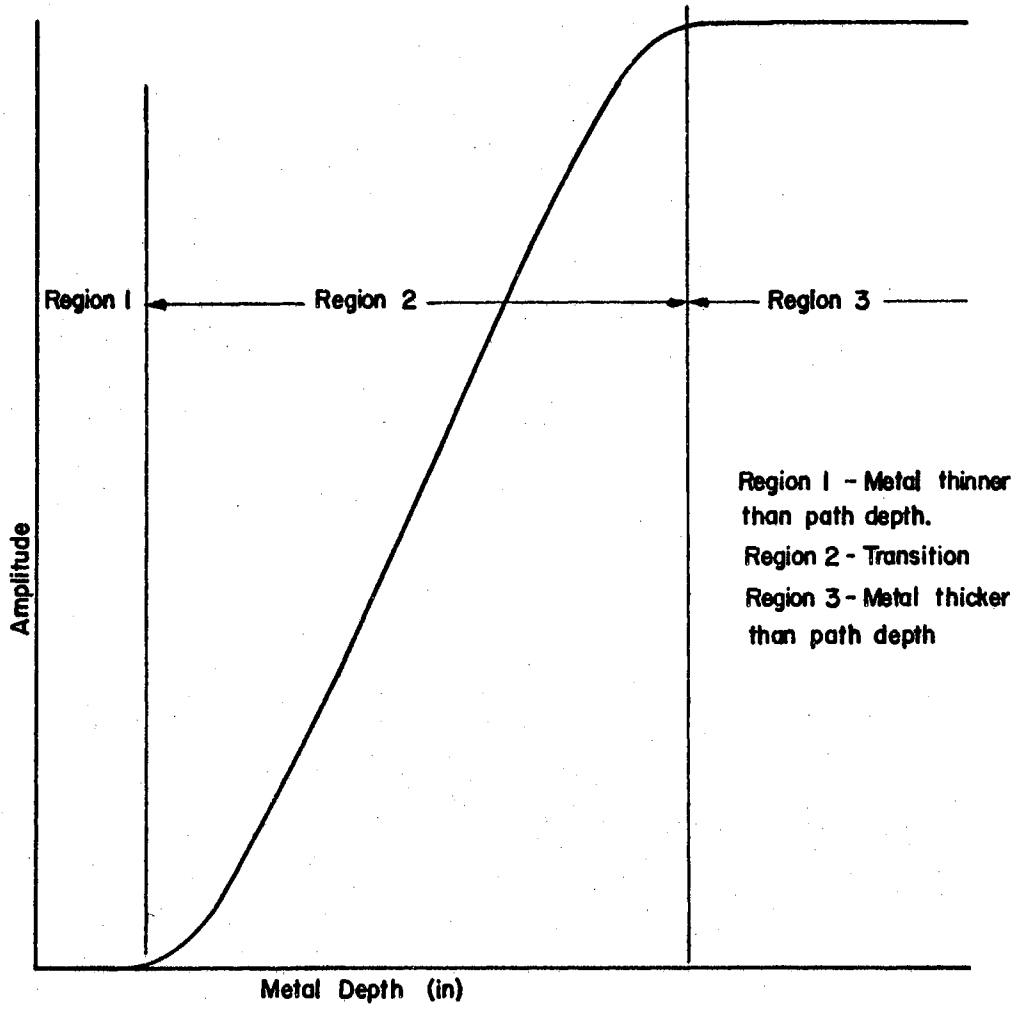

Figure 11. Typical Plot of Amplitude vs. Metal Depth

Each plot of the type shown in Figure 11 represents the amplitude of the signal versus metal depth for just one point along the path and it gives information about the depth of the path at that point. The data was normalized so that the maximum signal had an amplitude of ten corresponding to no obstruction in the path of the S-wave. Since there was some question about the exact location of the top and bottom of the path, it was decided to call the depth of the location of the path a single point corresponding to an amplitude of five. This point gave the approximate depth of the center of that portion of the wave which reached the receiver. A family of amplitude versus metal depth plots is shown in Figures 16, 17, 18 and 19 in the Appendix for just one path length.

A smooth line drawn through each depth point and connecting with zero depth points at each end where the wave entered and exited gave a plot of the wave path for a given distance between the transmitter and receiver (see Figure 12).

Similar curves were drawn for each of five different path lengths (see Figures 20, 21, 22, 23 and 24 in the Appendix). Superimposing the path plots onto one plot produced a family of paths which represents the direction of travel of the entire beam (see Figure 13).

Rather than thinking of each line in Figure 13 as a distinct path, the entire plot should be thought of as a field of a shear wave beam with the lines indicating the direction of travel of each portion of the beam.

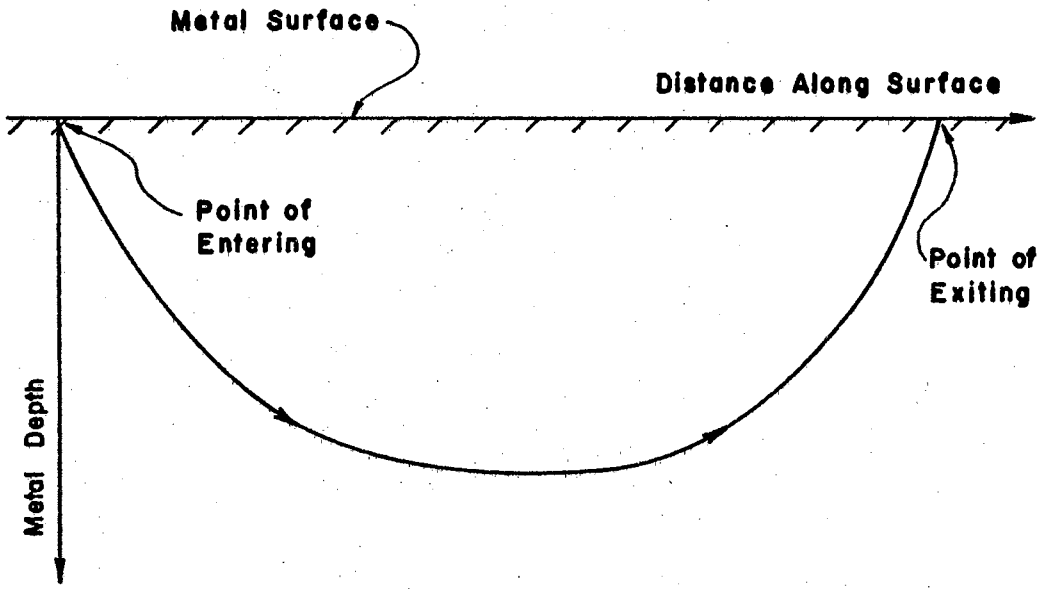

Figure 12. Typical S-Wave Path

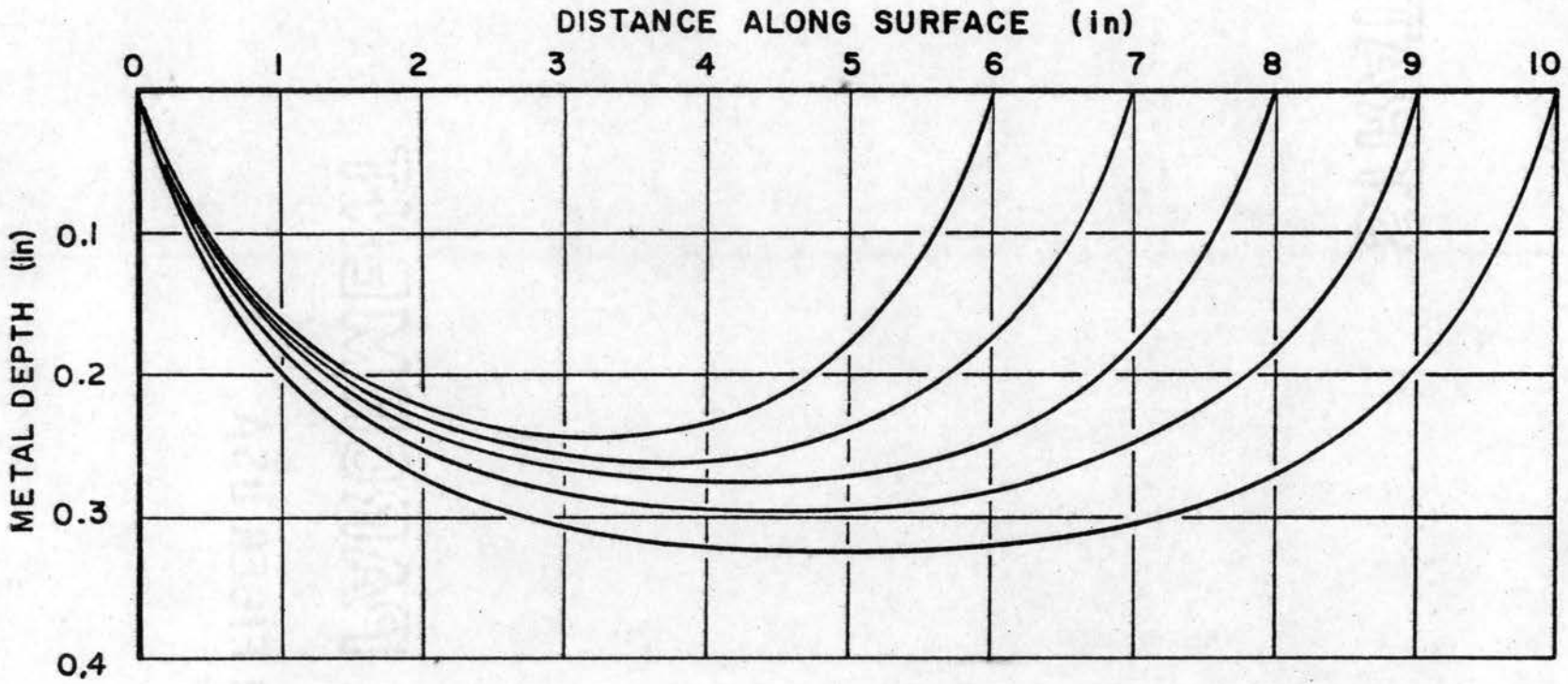

FIGURE 13. CURVING SHEAR WAVE BEAM

Discussion

All of the experimental observations can be explained by the beam shown in Figure 13. The angle of entering and of exiting for the wave can be measured from tangents to the curves at each end. The curves are symmetrical about the centers of the paths so that the angles at each end are the same, as was observed. The data was difficult to take near the ends of the paths because the transmitter and receiver were sitting almost directly over the saw cut and this caused additional signals which interfered with the S-wave signal. There was not enough data available near each end of the path to give a very accurate value for the angles, so the curves were drawn tangent on an angle which was calculated from Snell's law, Equation (1-1) and the known angle of incidence of the longitudinal wave in the Lucite block.

At the critical angle

$$\alpha_l = 66^\circ$$

$$\alpha_t = 90^\circ$$

Giving

$$\frac{c_t}{c_l} = \frac{\sin\alpha_t}{\sin\alpha_l} = \frac{\sin 90^\circ}{\sin 66^\circ} = 1.095$$

At maximum S-wave signal

$$\alpha_l = 57$$

Giving

$$\sin\alpha_t = \frac{c_t}{c_l}\sin\alpha_l = 1.095 \sin 57^\circ = 0.914$$

$$\alpha_t = 66^\circ$$

It can be seen from the paths that they did not have to be distorted to cause them to come in on a tangent to 66° from the vertical normal. All of the lines for each path are seen to enter and exit the surface at the same angle regardless of the path length.

The S-wave signal could not be damped on the surface between the transmitter and receiver simply because it was not present on the surface. In order to explain the new signals which were produced when damping was applied, it is necessary to say that the portion of the wave which strikes the surface between the transmitter and receiver is reflected and scattered so that practically none of it reaches the receiver. When damping is applied, some of this energy which strikes the boundary is converted into a Rayleigh surface wave and continues to the receiver in that form and produces a signal. It was found that when an ordinary straight shear wave is reflected from a boundary, some of the energy can be converted into a Rayleigh surface wave by applying damping at the point of reflection.

The constant ratio of the time required for the Rayleigh wave to the time required for the S-wave is explained by the fact that all of the path lines in Figure 13 have approximately the same shape. Also, the length of the paths are almost the same as the distance in a straight line between the two points. The large plots in Figures 20, 21, 22, 23, and 24 in the Appendix are plotted with the depth scale expanded ten times the distance scale, but the actual path shapes are plotted below each figure. These path are seen to be almost the same length as a line along the surface.

The resulting path plots are actually the only logical way to account for all of the experimental observations on the S-wave signal.

CHAPTER III

THEORETICAL CONSIDERATIONS

The mathematical formulation of this problem can be described without loss of generality as a pure shear wave entering an elastic half-space at some known angle. It is wished to impose these conditions plus the fact that the free surface of the half-space is unable to support any stress except tangentially to the surface. A solution to this problem should determine whether or not the shear wave can be made to curve for certain angles of entering due to the stress-free boundary conditions alone. The problem will be set up in this chapter, but no attempt will be made to solve the equations.

Approximations

Several well justified approximations can be made on this problem without losing a mathematical description of the actual physical problem. The approximations will be listed below.

1. The material through which the waves are propagated is perfectly homogeneous, isotropic and elastic.
2. The region of interest is a half-space with the exterior region a complete vacuum.
3. The only forces that are present are elastic and inertia forces.

4. The wave motion is two dimensional with no variation in the third space dimension.
5. There is no attenuation of energy in the elastic material.
6. The wave motion is purely sinusoidal with respect to time.

The first three approximations result from the use of a steel bar which was considerably thicker than the depth of the wave paths. The region adjacent to the bar was occupied by air at room conditions which affects the surface of steel almost exactly the same as a vacuum with respect to elastic waves. In steel, the elastic and inertia forces completely overwhelm any other forces which might be present, such as gravitational forces.

The experimental setup was such that only the distance between the transmitter and receiver and the metal depth were important space dimensions, leading to a two dimensional wave. Certainly some variation would be present in the lateral direction, but it is assumed that this variation did not affect the behavior of the waves which was of interest in this problem.

The last two assumptions are more difficult to justify, but by making them the problem is greatly reduced in complexity. Attenuation of energy is always present in any elastic wave propagation, but it is felt that the affects which might be caused by including this effect are not of interest in this problem. Conventionally, elastic waves are produced as pulses, but due to the simplification resulting from assumed sinusoidal motion, the first solution can be attempted with this assumption and hopefully meaningful results will be obtained.

Equations Describing Wave Motion

The equation of motion of an elemental volume in a solid is obtained by simply making a force balance between the elastic restoring forces and the inertia force. The elastic restoring forces are in terms of stresses which are related to the strains by Hooke's law. This results in the following equation which is called Navier's equation for a homogeneous isotropic elastic solid and is taken from Sokolnikoff (5).

$$\mu\nabla^2\tilde{u} + (\lambda+\mu)\nabla(\nabla\cdot\tilde{u}) + \rho p^2\tilde{u} = 0 \qquad (3\text{-}1)$$

Where

$\nabla = \left(\frac{\partial}{\partial x}, \frac{\partial}{\partial y}\right)$, the vector operator "del"

$\nabla^2 = \nabla\cdot\nabla = \frac{\partial^2}{\partial x^2} + \frac{\partial^2}{\partial y^2}$

x and y are the space coordinates

$\tilde{u}(x,y)e^{-ipt}$ is the displacement vector (see Figure 14)

u and v are the components of the displacement vector

ρ is the density of the solid

p is the angular frequency

μ and λ are Lame' constants

Lame' constants are related to Young's modulus "E" and Poisson's ratio "σ" by,

$$\mu = \frac{E}{2(1+\sigma)}, \qquad \lambda = \frac{E\sigma}{(1+\sigma)(1-2\sigma)}.$$

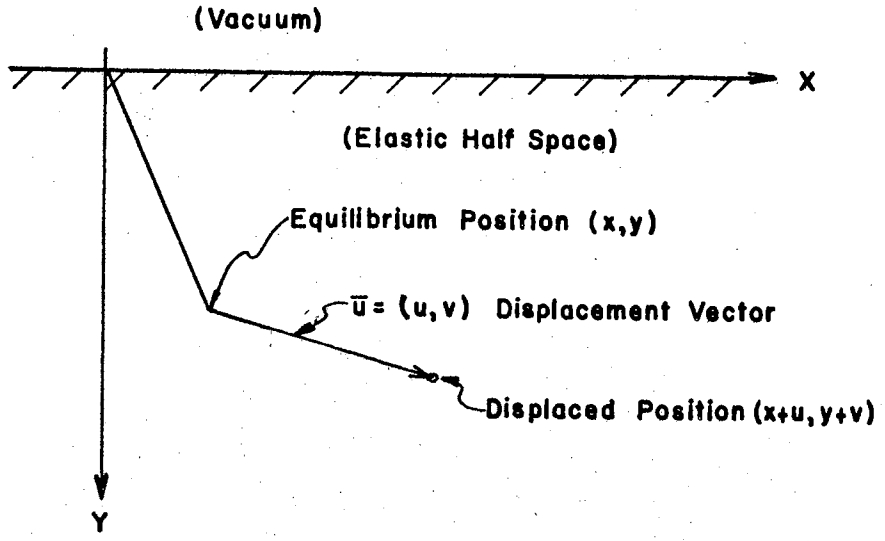

Figure 14. Half-Space and Displacement Vector

Expanding Equation (3-1) into two equations by taking the partial derivatives.

$$\mu\left(\frac{\partial^2 u}{\partial x^2} + \frac{\partial^2 u}{\partial y^2}\right) + (\lambda+\mu)\frac{\partial}{\partial x}\left(\frac{\partial u}{\partial x} + \frac{\partial v}{\partial y}\right) + \rho p^2 u = 0 \qquad (3\text{-}2)$$

$$\mu\left(\frac{\partial^2 v}{\partial x^2} + \frac{\partial^2 v}{\partial y^2}\right) + (\lambda+\mu)\frac{\partial}{\partial y}\left(\frac{\partial u}{\partial x} + \frac{\partial v}{\partial y}\right) + \rho p^2 v = 0 \qquad (3\text{-}3)$$

Rearranging the terms in Equations (3-2) and (3-3).

$$(\lambda+2\mu)\frac{\partial}{\partial x}\left(\frac{\partial u}{\partial x} + \frac{\partial v}{\partial y}\right) - \mu\frac{\partial}{\partial y}\left(\frac{\partial v}{\partial x} - \frac{\partial u}{\partial y}\right) + \rho p^2 u = 0 \qquad (3\text{-}4)$$

$$(\lambda+2\mu)\frac{\partial}{\partial y}\left(\frac{\partial u}{\partial x} + \frac{\partial v}{\partial y}\right) + \mu\frac{\partial}{\partial x}\left(\frac{\partial v}{\partial x} - \frac{\partial u}{\partial y}\right) + \rho p^2 v = 0 \qquad (3\text{-}5)$$

Defining the dilatation "Δ" and rotation "Ω" as,

$$\Delta = \frac{\partial u}{\partial x} + \frac{\partial v}{\partial y}, \qquad \Omega = \tfrac{1}{2}\left(\frac{\partial v}{\partial x} - \frac{\partial u}{\partial y}\right), \qquad (3\text{-}6)$$

Giving,

$$(\lambda+2\mu)\frac{\partial\Delta}{\partial x} - 2\mu\frac{\partial\Omega}{\partial y} + \rho p^2 u = 0 \tag{3-7}$$

$$(\lambda+2\mu)\frac{\partial\Delta}{\partial y} + 2\mu\frac{\partial\Omega}{\partial x} + \rho p^2 v = 0 \tag{3-8}$$

Differentiating Equation (3-7) with respect to "x" and Equation (3-8) with respect to "y" and adding the resulting equations,

$$(\lambda+2\mu)\left(\frac{\partial^2}{\partial x^2} + \frac{\partial^2}{\partial y^2}\right)\Delta + \rho p^2\left(\frac{\partial u}{\partial x} + \frac{\partial v}{\partial y}\right) = 0$$

Substituting from Equation (3-6),

$$(\lambda+2\mu)\nabla^2\Delta + \rho p^2\Delta = 0 \tag{3-9}$$

Differentiating Equation (3-8) with respect to "x" and Equation (3-7) with respect to "y" and subtracting the resulting equations,

$$2\mu\left(\frac{\partial^2}{\partial x^2} + \frac{\partial^2}{\partial y^2}\right)\Omega + \rho p^2\left(\frac{\partial v}{\partial x} - \frac{\partial u}{\partial y}\right) = 0$$

Substituting from Equation (3-6),

$$\mu\nabla^2\Omega + \rho p^2\Omega = 0 \tag{3-10}$$

The dilatation is associated with a longitudinal wave and the rotation with a shear wave. If $\Delta = 0$ then the wave is a shear wave. The wave of interest in this problem is initially a shear wave, but this is no insurance that the wave will remain purely shear when it is very near the surface. For this reason, solutions need to be obtained for both the dilatation and rotation.

Defining,

$$c_l = \left(\frac{\lambda+2\mu}{\rho}\right)^{\frac{1}{2}}, \text{ longitudinal wave velocity}$$

$$c_t = (\mu/\rho)^{\frac{1}{2}}, \text{ shear wave velocity}$$

$$k_l = p/c_l, \quad k_t = p/c_t \tag{3-11}$$

Substituting the quantities from Equation (3-11) into Equation (3-9) and (3-10),

$$(\nabla^2+k_l^2)\Delta = 0 \tag{3-12}$$

$$(\nabla^2+k_t^2)\Omega = 0 \tag{3-13}$$

Equations (3-12) and (3-13) are called Helmholtz equations for two dimensions. Solutions for these equations would be substituted into Equations (3-7) and (3-8) to give solution for "u" and "v", the components of the displacement vector.

Boundary Conditions

A very important part of this problem is imposing the correct boundary conditions on the solution. The boundary conditions will be listed here and explained.

The conditions, that the wave be pure shear and traveling a certain direction when it enters the material, imposes two requirements on the wave at the point of entering. They are that $\Delta = 0$ at $(x, y) = (0, 0)$, the condition for pure shear, and that $v/u = -\tan\theta_o$ at $(x, y) = (0, 0)$, the direction condition. It should be noted that the shear wave particle motion is transverse to the direction of wave propagation.

The other conditions to which the wave must conform at the boundary are the stress conditions. Since the elastic half-space is bounded only by a vacuum, it is unable to support normal stress and shearing stress at the boundary. This can be stated in the equations

$$\tau_{yy}(x, 0) = 0, \qquad \tau_{xy}(x, 0) = 0 \tag{3-14}$$

From Sokolnikoff (5), the stress tensor is given by Hooke's law,

$$\tau_{\alpha\beta} = \lambda\delta_{\alpha\beta}\left(\frac{\partial u}{\partial x} + \frac{\partial v}{\partial y}\right) + 2\mu e_{\alpha\beta} \quad (\alpha,\beta = 1,2) \tag{3-15}$$

Where

$$\tau_{11} = \tau_{xx} \qquad \tau_{12} = \tau_{xy} \qquad \tau_{22} = \tau_{yy}$$

$$\delta_{\alpha\beta} = \begin{matrix} 1 \text{ if } \alpha = \beta \\ 0 \text{ if } \alpha \neq \beta \end{matrix}$$

$$e_{22} = \frac{\partial v}{\partial y}, \qquad e_{12} = \tfrac{1}{2}\left(\frac{\partial u}{\partial y} + \frac{\partial v}{\partial x}\right)$$

This gives

$$\tau_{yy} = (\lambda+2\mu)\frac{\partial v}{\partial y} + \lambda\frac{\partial u}{\partial x} \tag{3-16}$$

$$\tau_{xy} = \mu\left(\frac{\partial u}{\partial y} + \frac{\partial v}{\partial x}\right) \tag{3-17}$$

Substituting Equations (3-16) and (3-17) into Equation (3-14) gives,

$$(\lambda+2\mu)\,\frac{\partial v(x,0)}{\partial y} + \lambda\frac{\partial u(x,0)}{\partial x} = 0 \tag{3-18}$$

$$\frac{\partial u(x,0)}{\partial y} + \frac{\partial v(x,0)}{\partial x} = 0 \tag{3-19}$$

These boundary conditions are illustrated in Figure 15.

Summarizing the boundary conditions:

1. $\Delta(0,0) = \dfrac{\partial u(0,0)}{\partial x} + \dfrac{\partial v(0,0)}{\partial y} = 0$
2. $v(0,0) + u(0,0)\tan\theta_0 = 0$
3. $(\lambda+2\mu)\dfrac{\partial v(x,0)}{\partial y} + \lambda\dfrac{\partial u(x,0)}{\partial x} = 0$
4. $\dfrac{\partial u(x,0)}{\partial y} + \dfrac{\partial v(x,0)}{\partial x} = 0$

In order to get a description for the shear wave path, any solution for the components "u" and "v" of the displacement vector must satisfy the four conditions listed.

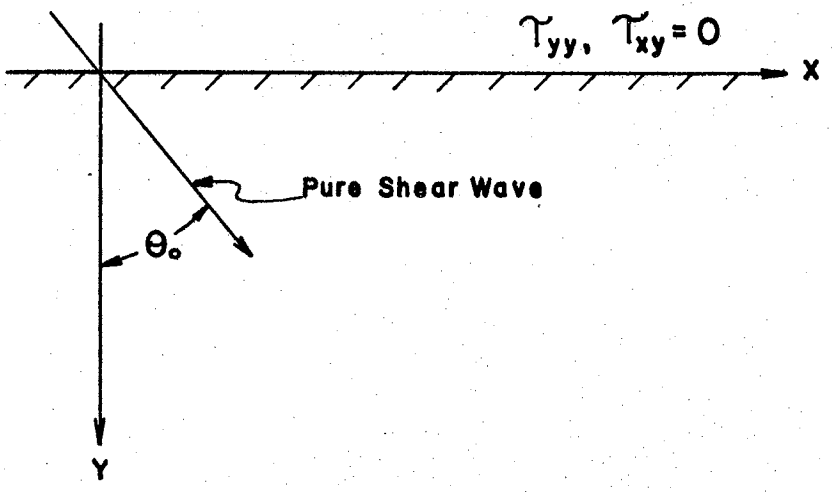

Figure 15. Boundary Conditions

CHAPTER IV

CONCLUSIONS AND RECOMMENDATIONS

Conclusions

The experimental results presented in Chapter II show that this wave is being affected by the free boundary by being curved back into the surface. Referring to the actual path shapes in Figures 20, 21, 22, 23 and 24 in the Appendix, it is seen that the curvature of the path is almost entirely at each end with the center portion of the path being almost parallel to the surface.

This wave is seen to be present only for one angle of refraction of the shear wave which was approximately 57°. When this angle was increased, most of the energy went into a Rayleigh surface wave, and when the angle was decreased, most of the energy went into a regular straight shear wave.

This wave is called a shear wave simply because it enters the material as a shear wave. One possibility is that the wave travels the entire path as a shear wave and the other possibility is that a component of dilatation becomes present in the wave. It is possible that the fact that it does not remain as a shear wave is the reason that it does curve.

The main conclusions from this study is that the mathematical equations need to be solved in order to provide further evidence to support the experimental findings given here. A good mathematical solution would probably give much more insight into the exact behavior of this wave and the reasons for its behavior.

Recommendations

The most obvious recommendation is that the problem as presented in Chapter III be solved. Several methods of solution were attempted without success by this author. Although a solution was not obtained, some recommendations will be made about an approach to a solution. The half-space region immediately suggests a transform type solution or an integral solution. Several transforms were attempted with both rectangular and cylindrical coordinates and the first difficulty was matching the boundary conditions and the second difficulty was, of course, obtaining the inverse transform.

The method of Green's Functions appeared to be ideal for solving the system of Helmholtz equations given in Equations (3-12) and (3-13). This method led to a set of integral equations which presented the same problem as inverting the transforms.

It is felt that a transform solution could be made to meet the boundary conditions, and if these boundary conditions are responsible for the curvature of the wave path, the solution would supply the needed information.

The importance of a mathematical solution cannot be over stressed and the experimental conclusions for the problem would be greatly strengthened by mathematical agreement.

SELECTED BIBLIOGRAPHY

1. Redwood, M. Mechanical Wave Guides. The MacMillan Company, New York, 1960, p. 44.

2. Rasmussen, J. G. "Prediction of Fatigue Failure Using Ultrasonic Surface Waves," Nondestructive Testing, Vol. XX, No. 2, March-April, 1962, p. 106.

3. Daniel, J. A. "Development of an Ultrasonic Surface Wave Testing Standard," (M. S. Thesis, Oklahoma State University, 1963,) pp. 6-7.

4. Rayleigh. "On Waves Propagated along the Plane Surface of an Elastic Solid," Proceedings of the London Mathematical Society, Vol. 17, 1887.

5. Sokolnikoff, I. S. Mathematical Theory of Elasticity, McGraw-Hill Book Co., Inc., New York, 1956, pp. 71-73, 370-376.

GENERAL BIBLIOGRAPHY

1. Cagniard, L. Reflection and Refraction of Progressive Seismic Waves, McGraw-Hill Book Co., Inc., New York, 1962.

2. Fredicks, R. W. and L. Knopoff. "The Reflection of Rayleigh Waves by a High Impedence Obstacle on a Half-Space," Geophysics, Vol. XXV, No. 6, Dec., 1960.

3. Jones, O. E. and A. T. Ellis. "Longitudinal Strain Pulse Propagation in Wide Rectangular Bars," Journal of Applied Mechanics, Vol. 30, Series E, No. 1, March, 1963.

4. Kolsky, H. Stress Waves in Solids, Oxford University Press, London, 1953.

5. Lindsay, R. B. Mechanical Radiation, McGraw-Hill Book Co., Inc., New York, 1960.

6. Morse, P. M. and H. Feshbach. Methods of Theoretical Physics Part I and II, McGraw-Hill Book Co., Inc., New York, 1953.

7. Sneddon, I. N. Elements of Partial Differential Equations, McGraw-Hill Book Co., Inc., New York, 1957.

APPENDIX

APPENDIX

Several plots will be given in the following figures in order to illustrate how Figure 13 was obtained. Figures 16, 17, 18 and 19 give the Amplitude versus Metal Thickness plots for several positions along the nine inch path. Figures 20, 21, 22, 23 and 24 give the wave path shapes for each path length on which data was taken. In each of these figures a small plot of the actual path shape is given at the bottom of the page. On these plots, both the ordinate and abscissa are on the same scale, enabling the actual shape of the wave travel to be visualized.

Two quantities will be defined which are used in the plots.

D = distance from point of entering to point of exiting

x = distance from point of entering to some point along the path

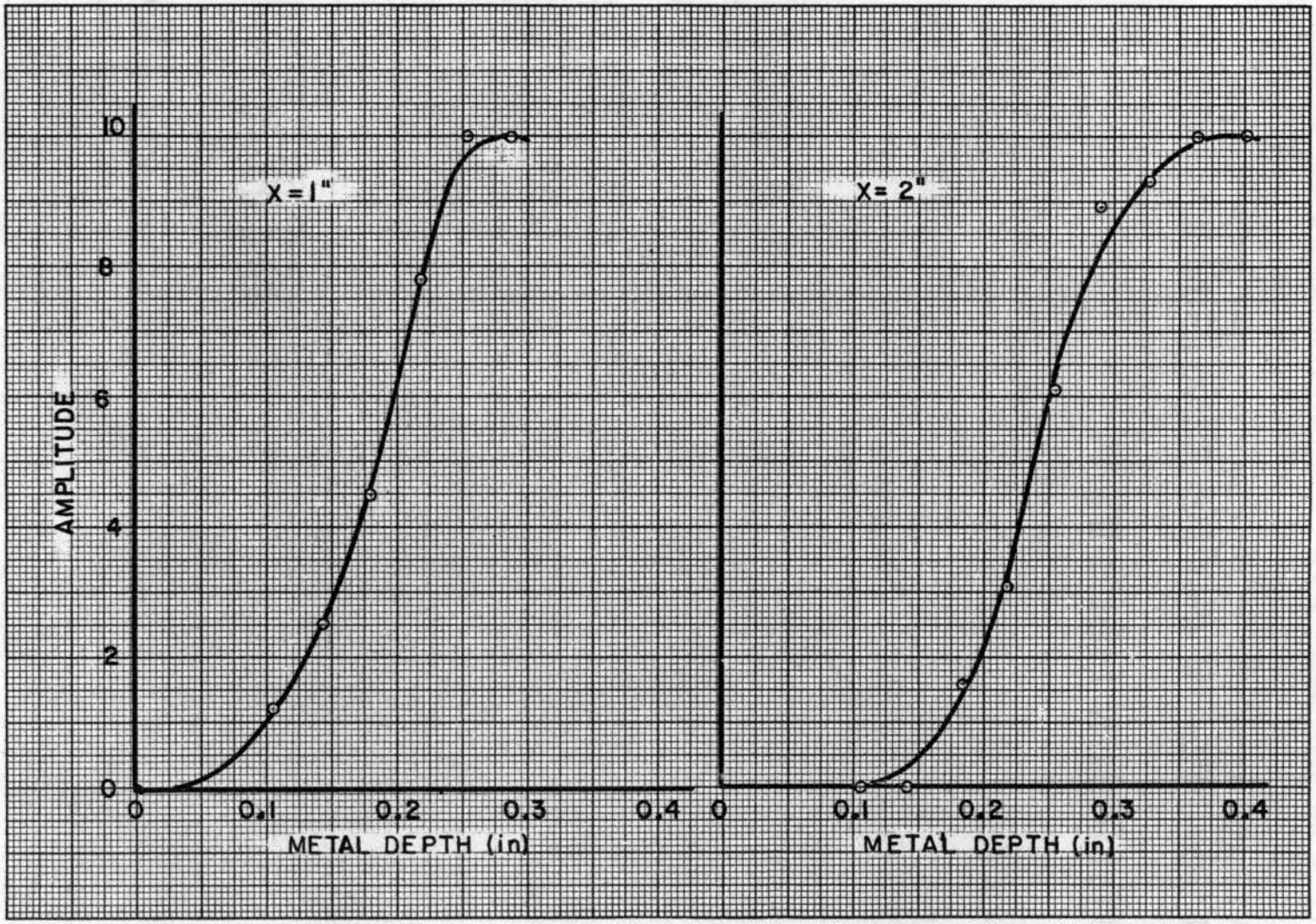

FIG. NO. 16 AMPLITUDE VS. METAL DEPTH D=9"

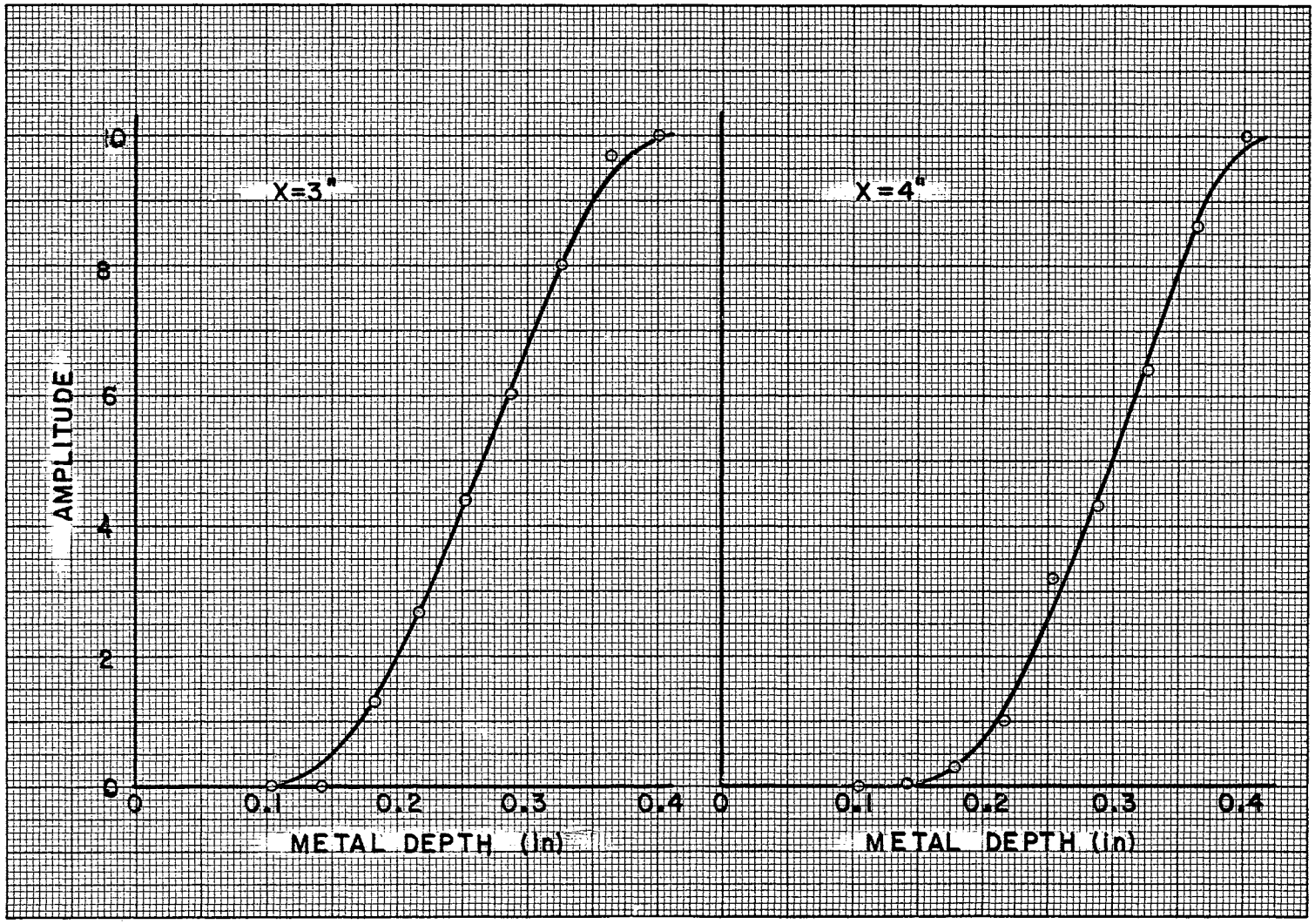

FIG. NO. 17 AMPLITUDE VS. METAL DEPTH D=9"

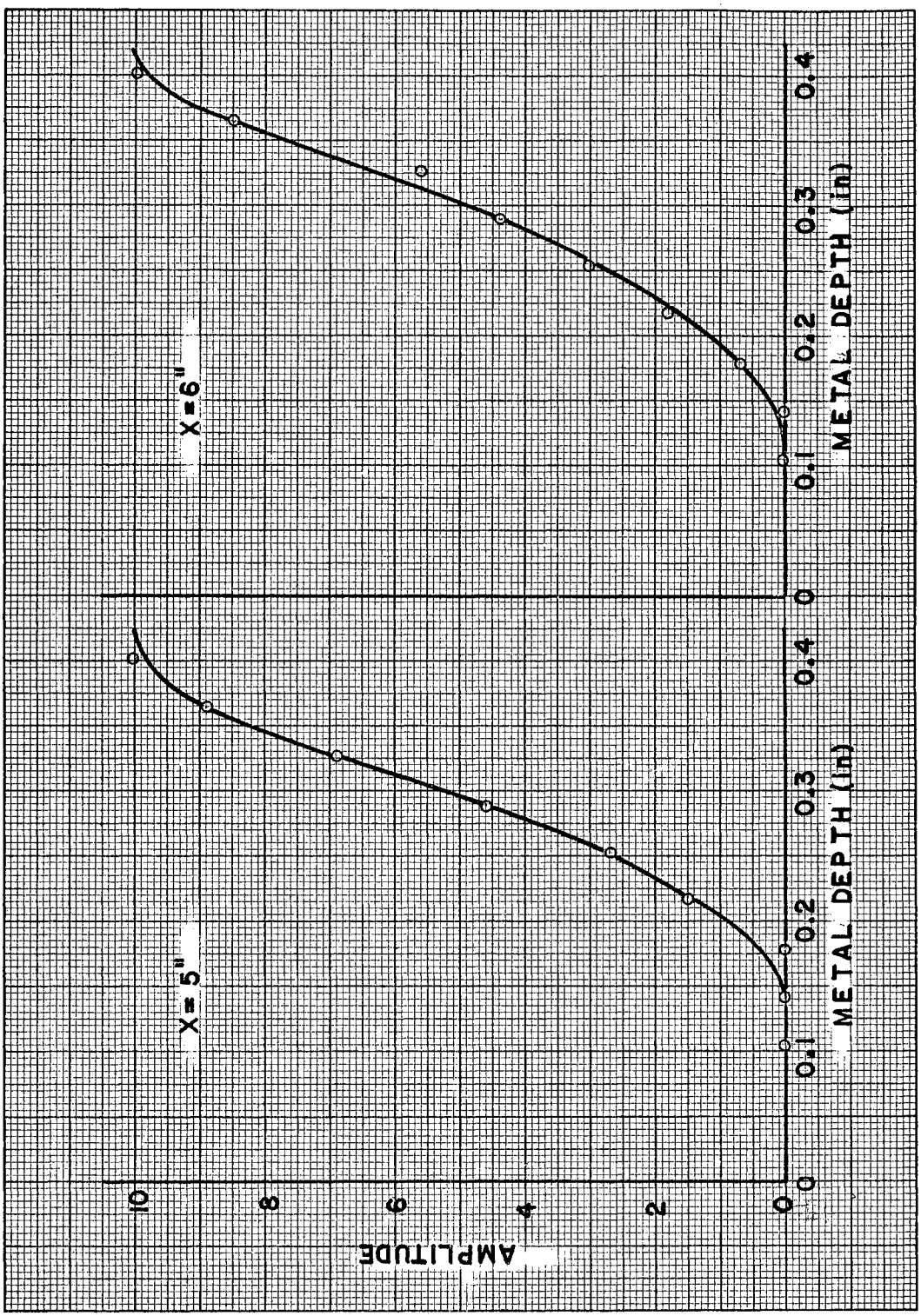

FIG. NO. 18 AMPLITUDE VS. METAL DEPTH D = 9"

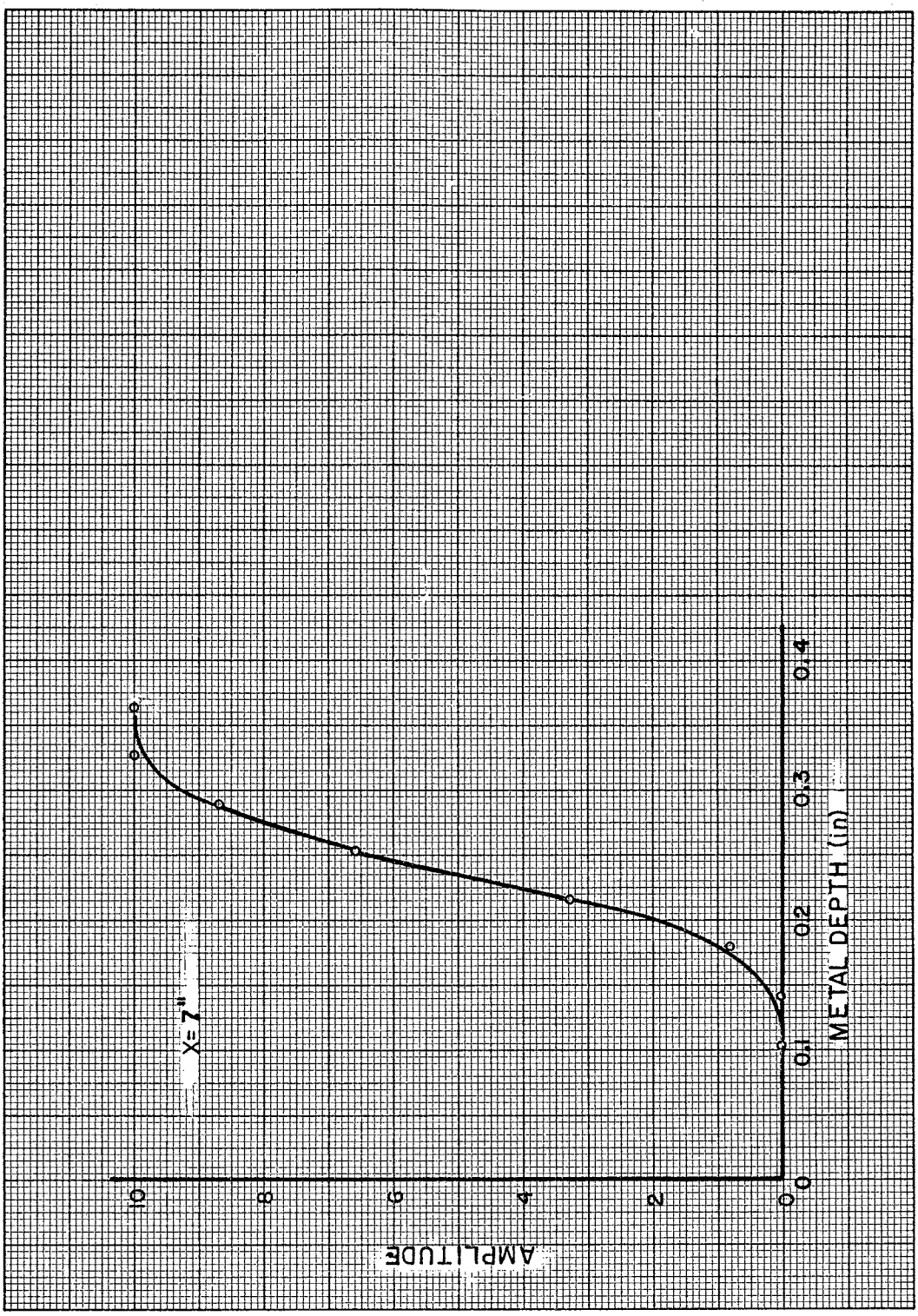

FIG. NO. 19 AMPLITUDE VS. METAL DEPTH D=9"

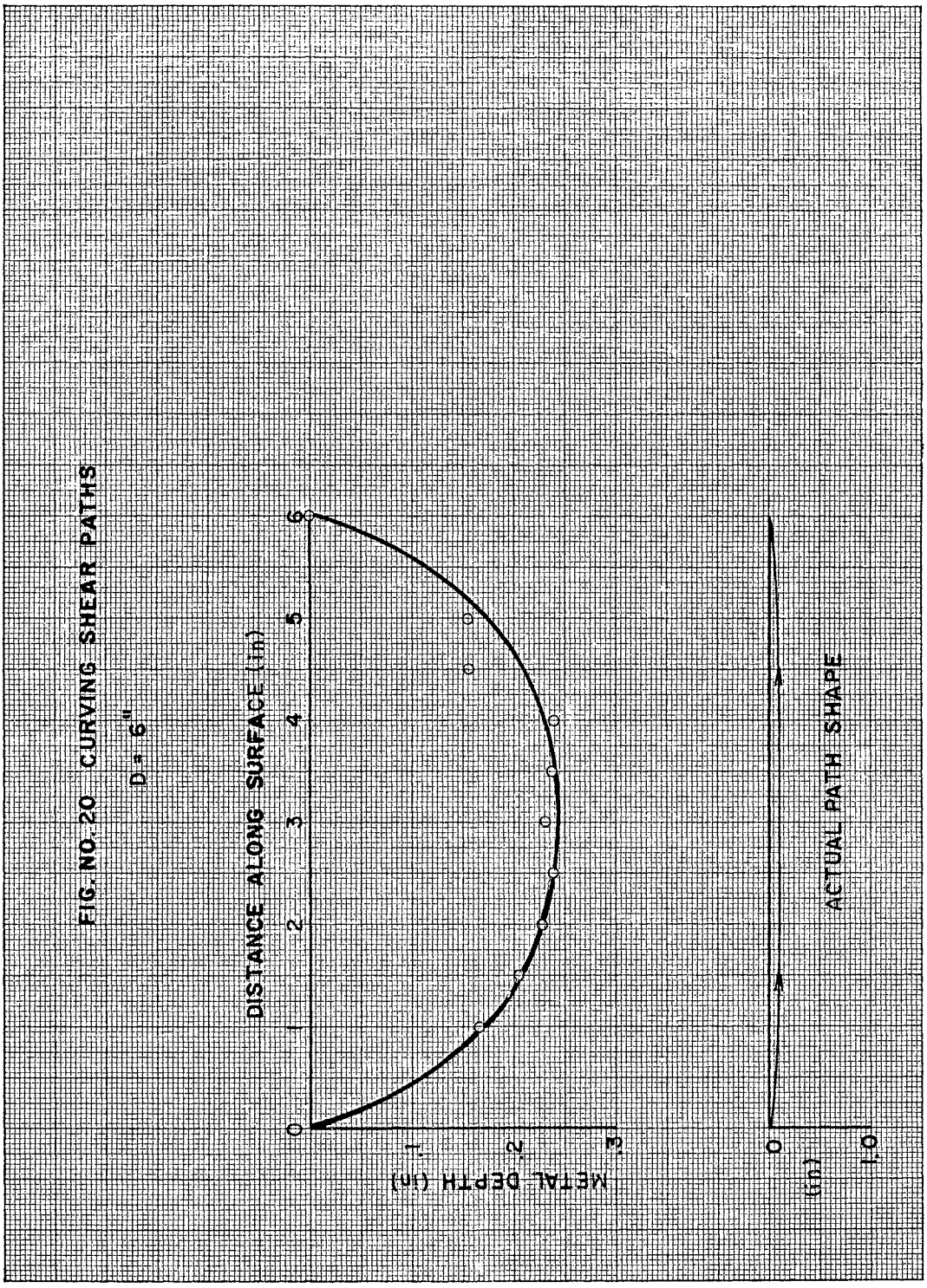
FIG. NO. 20 CURVING SHEAR PATHS
D = 6"
DISTANCE ALONG SURFACE (in.)
0
1
2
3
4
5
6
METAL DEPTH (in)
1
2
3
ACTUAL PATH SHAPE
0
(in.)
1.0

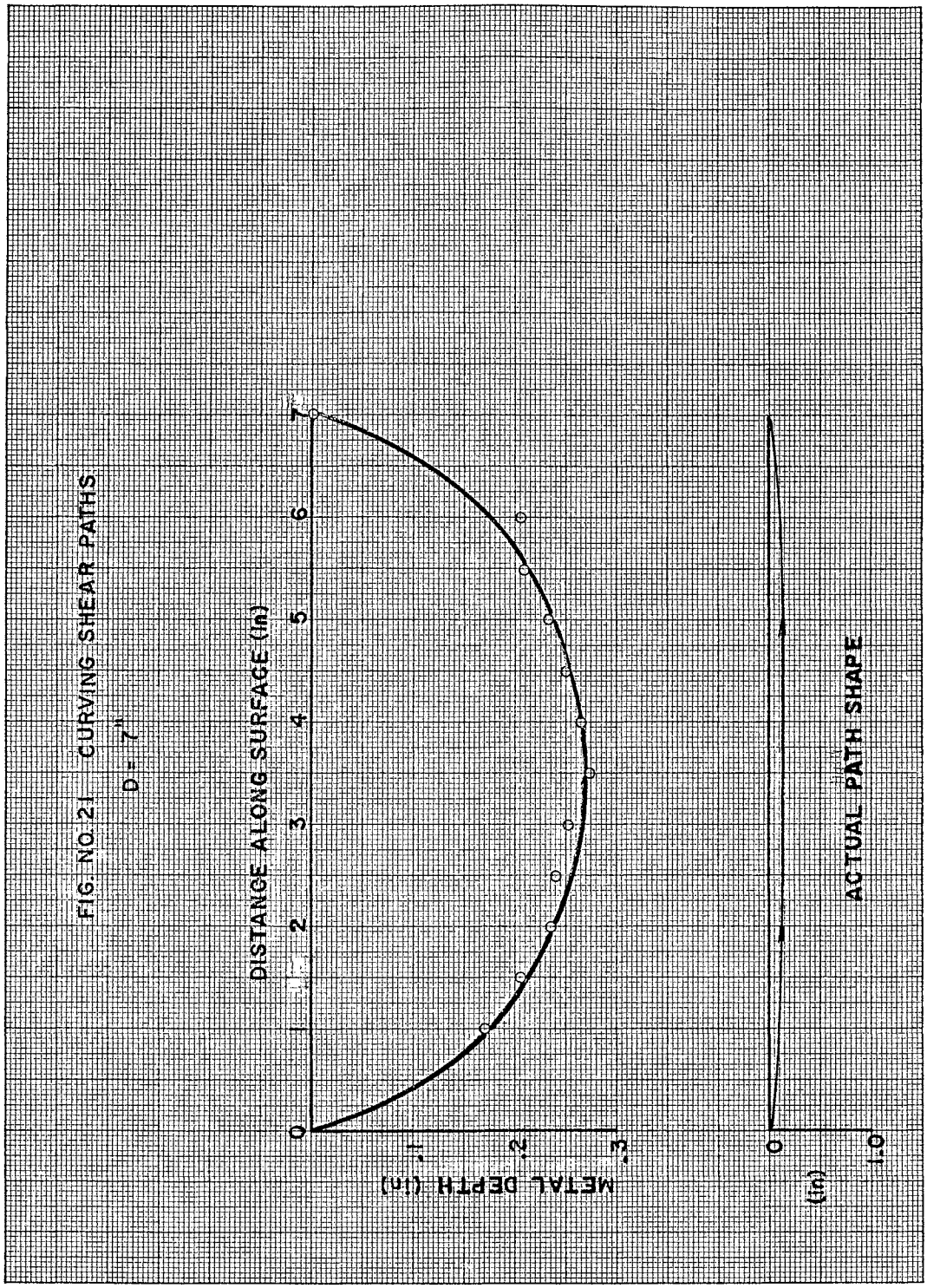

FIG. NO. 21 CURVING SHEAR PATHS
D = 7"

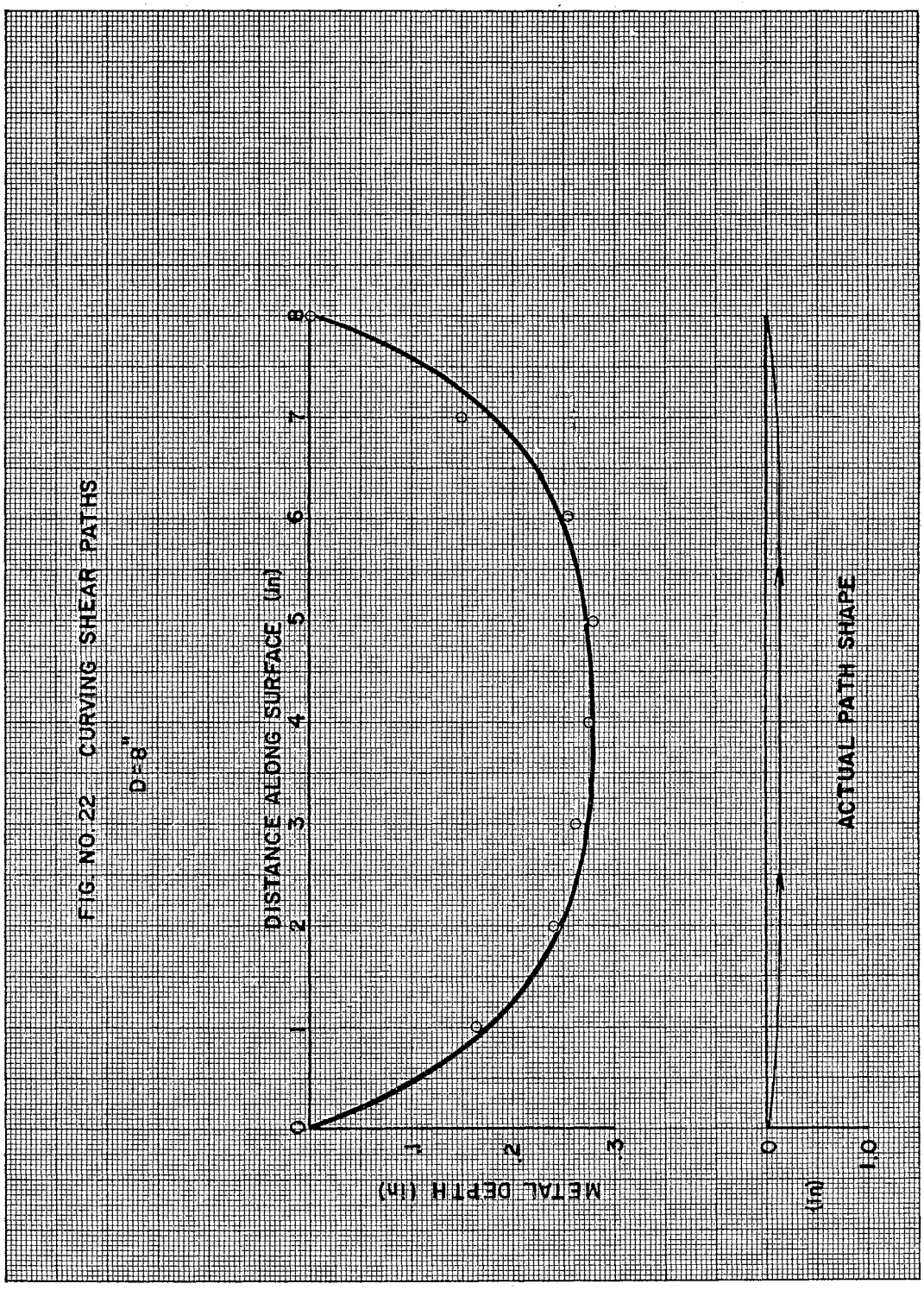
FIG. NO. 22 CURVING SHEAR PATHS
D=8"
DISTANCE ALONG SURFACE (in)
METAL DEPTH (in)
ACTUAL PATH SHAPE
(in)

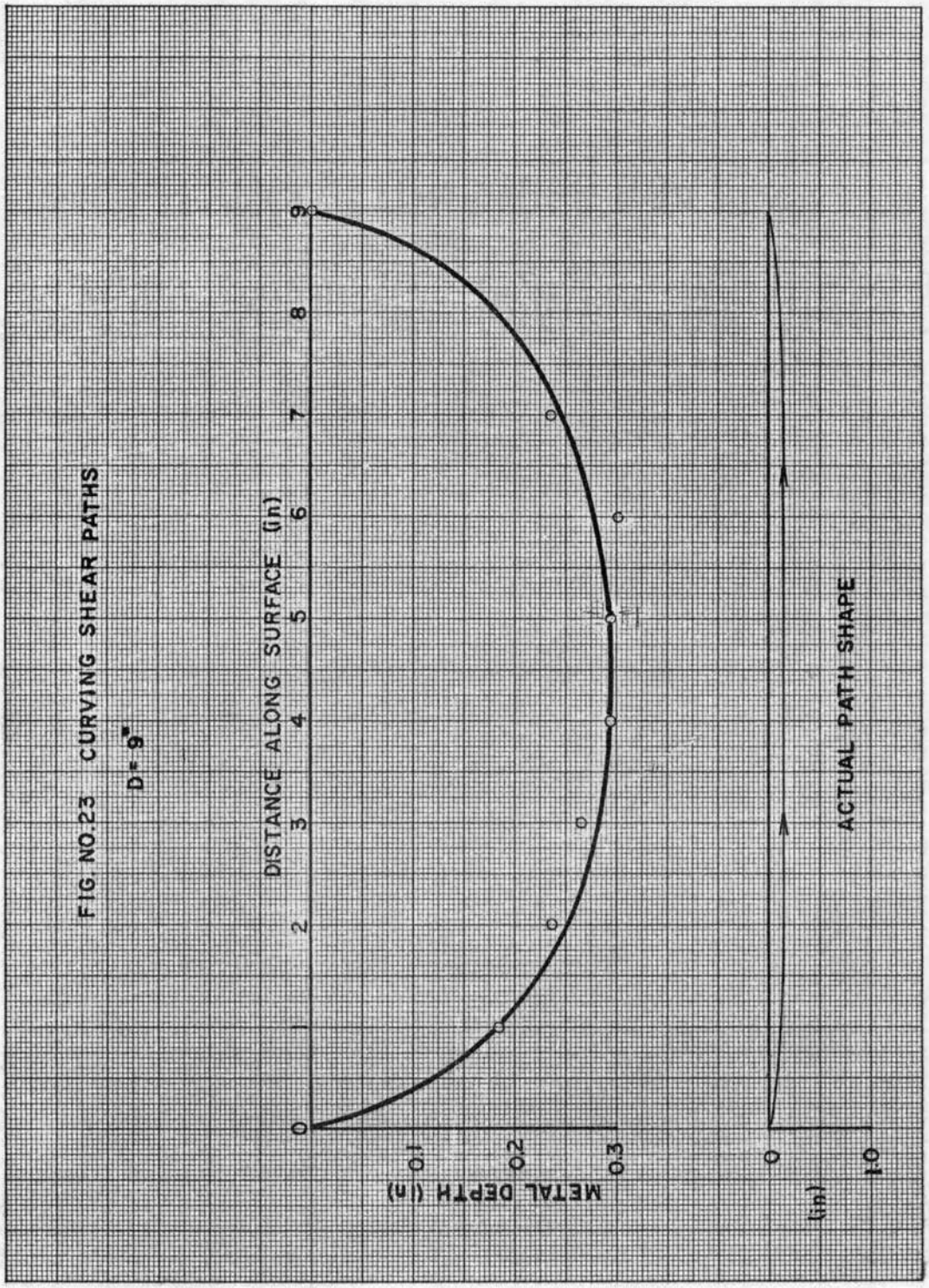
FIG. NO.23 CURVING SHEAR PATHS
D = 9"
DISTANCE ALONG SURFACE (in)
0
1
2
3
4
5
6
7
8
9
METAL DEPTH (in)
0.1
0.2
0.3
ACTUAL PATH SHAPE
0
(in)
1.0

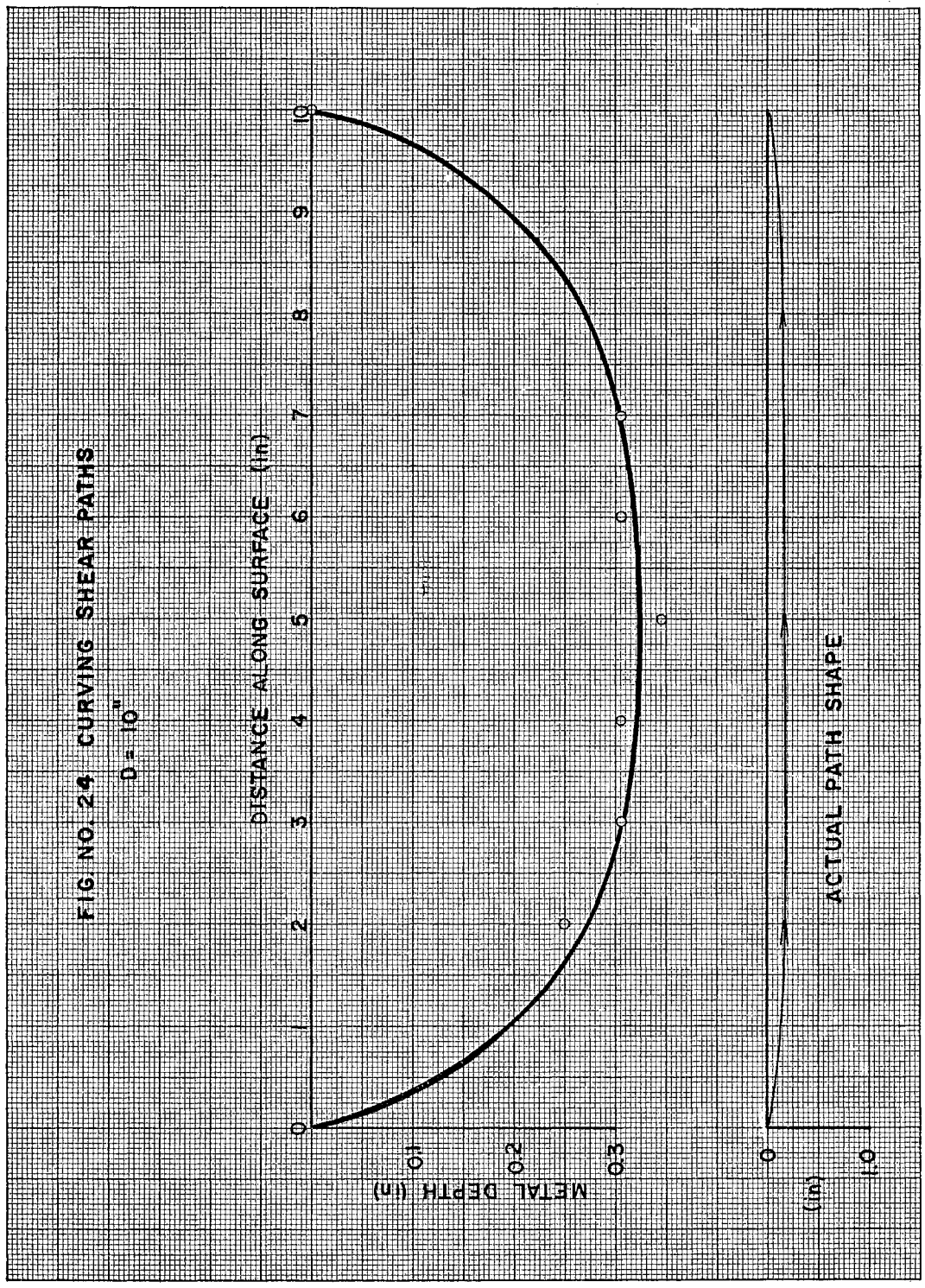
FIG. NO. 24 CURVING SHEAR PATHS
D = 10"
DISTANCE ALONG SURFACE (in)
0
1
2
3
4
5
6
7
8
9
10
METAL DEPTH (in)
0.1
0.2
0.3
ACTUAL PATH SHAPE
0
1.0
(in)

VITA

Philip Wayne Randles

Candidate for the Degree of

Master of Science

Thesis: THE BEHAVIOR OF ELASTIC WAVES NEAR A FREE BOUNDARY

Major Field: Mechanical Engineering

Biographical:

Personal Data: Born in Guymon, Oklahoma, May 11, 1939, the son of James and Bess Randles.

Education: Panhandle A & M College, Goodwell, Oklahoma, 1957-59; Oklahoma State University, Stillwater, Oklahoma, 1959-63; received the Bachelor of Science degree in May, 1962, Oklahoma State University; completed the requirements for the Master of Science degree in August, 1963, Oklahoma State University.

Professional Organizations: The American Society of Mechanical Engineers.